

## Spectroscopic properties and reactivity of a mononuclear oxomanganese(IV) complex†

Domenick F. Leto, Rena Ingram, Victor W. Day and Timothy A. Jackson\*

Cite this: *Chem. Commun.*, 2013, **49**, 5378Received 10th January 2013,  
Accepted 25th April 2013

DOI: 10.1039/c3cc00244f

www.rsc.org/chemcomm

**A non-porphyrinic, mononuclear oxomanganese(IV) complex was generated at room temperature and characterized by spectroscopic methods. The Mn<sup>IV</sup>=O adduct is capable of activating C–H bonds by a H-atom transfer mechanism and is more reactive in this regard than most Mn<sup>IV</sup>=O species.**

High-valent oxomanganese adducts are suggested as active oxidants for synthetic and biological manganese catalysts, including those involved in textile and paper bleaching with H<sub>2</sub>O<sub>2</sub> and oxygen evolution from water.<sup>1</sup> Oxomanganese(v) adducts with *S* = 0 and 1 spin states have been reported, and these invariably feature strongly electron-donating, anionic ligands.<sup>2</sup> Oxomanganese(IV) complexes with neutral, non-porphyrinic ligands are comparatively less common.<sup>3</sup> Detailed studies of substrate oxidation exist for a limited number of complexes.<sup>3a-c,4</sup> In addition, few Mn<sup>IV</sup>=O complexes have been characterized by Mn K-edge X-ray absorption spectroscopy (XAS),<sup>3b,5</sup> a technique featuring prominently in the study of Mn enzymes<sup>1b</sup> and biominerals.<sup>6</sup> In this report, we describe the spectroscopic properties and oxidative reactivity of an oxomanganese(IV) complex supported by the neutral, pentadentate N4py ligand (*N,N*-bis(2-pyridylmethyl)-*N*-bis(2-pyridyl)methylamine). This Mn<sup>IV</sup>=O compound is more reactive than the majority of Mn<sup>IV</sup>=O complexes for C–H bond oxidation.

The manganese(II) complex [Mn<sup>II</sup>(N4py)]<sup>2+</sup> (**1**) was generated as the triflate salt. The X-ray diffraction (XRD) structure exhibits a distorted octahedral Mn<sup>II</sup> center with pentadentate N4py and monodentate triflate ligands (Fig. 1A). The Mn–ligand bond lengths are 2.1 to 2.3 Å. The Mn K-edge XAS spectrum of a frozen aqueous sample of **1**(OTf)<sub>2</sub> displays a pre-edge feature at 6540.6 eV and an edge at 6547.3 eV. The EXAFS data are best fit with 1 O at 2.09 Å, 5 N at 2.26 Å, and 3 C at 3.00 Å, in excellent agreement with the XRD structure (*cf.* Tables S4 and S6; ESI†).

The addition of excess PhIO (2.5 equiv.) to **1** in CF<sub>3</sub>CH<sub>2</sub>OH at 298 K led to the formation of a green species (**2**), with a broad

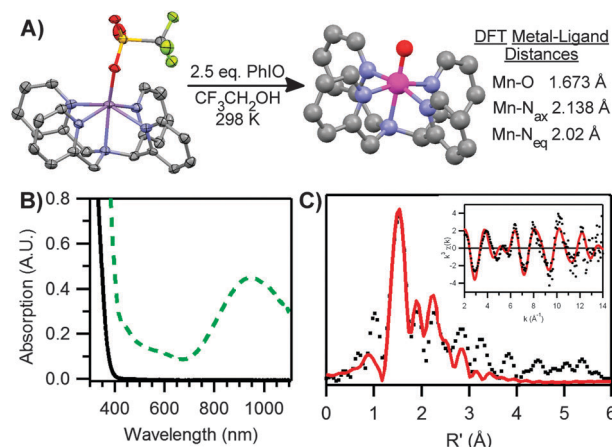


**Fig. 1** (A) XRD structure of [Mn<sup>II</sup>(N4py)(OTf)]<sup>+</sup> (**1**(OTf), left) and DFT (BP/TZVP) structure of [Mn<sup>IV</sup>(O)(N4py)]<sup>2+</sup> (**2**, right). Hydrogen atoms are omitted for clarity. (B) 298 K electronic absorption spectra of **1** (black solid trace) and **2** (green dashed trace); both 2 mM in CF<sub>3</sub>CH<sub>2</sub>OH. (C) Fourier transform of the Mn K-edge EXAFS data and EXAFS spectrum (inset), experimental data (···) and fits (–), for **2** in CF<sub>3</sub>CH<sub>2</sub>OH.

electronic absorption band at 950 nm and weaker features at 600 and 450 nm (Fig. 1B). At 298 K, the formation of **2** finished in ~10 minutes, and **2** showed a half-life of 30 minutes. The absorption features of **2** are very similar to those of other non-porphyrinic Mn<sup>IV</sup>=O complexes in tetragonal, six-coordinate environments, which display broad near-infrared bands from ~1040–825 nm and weaker features at higher energies.<sup>3a,b,7</sup> The perpendicular mode X-band EPR spectrum of **2** is typical of a mononuclear, *S* = 3/2 Mn<sup>IV</sup> ion (Fig. S4; ESI†).<sup>3a,b,d,8</sup> Hyperfine coupling for the *g*<sub>eff</sub> = 5.76 feature is ~76 G, in good agreement with that observed for other Mn<sup>IV</sup>=O complexes.<sup>3d</sup> High-resolution electrospray-ionization mass spectral (ESI-MS) data of **2** reveal a major ion peak at *m/z* 219.0502, consistent with [Mn<sup>IV</sup>(O)(N4py)]<sup>2+</sup> (*m/z* calc. 219.0563). When **2** is spiked with 10 μL H<sub>2</sub><sup>18</sup>O (97% <sup>18</sup>O-enriched), a new molecular ion peak is observed at *m/z* 220.0537, indicating incorporation of <sup>18</sup>O from H<sub>2</sub><sup>18</sup>O ([Mn<sup>IV</sup>(<sup>18</sup>O)(N4py)]<sup>2+</sup> *m/z* calc. 220.0585). These data together support the formulation of **2** as [Mn<sup>IV</sup>(O)(N4py)]<sup>2+</sup>.

As we have been unable to grow crystals of **2**, its molecular structure was investigated by Mn K-edge XAS. The edge energy

Department of Chemistry, The University of Kansas, 1251 Wescoe Hall Drive, Lawrence, KS, USA. E-mail: taj@ku.edu; Fax: +1-785-864-5396; Tel: +1-785-864-3968

† Electronic supplementary information (ESI) available: Details of experimental and kinetic procedures. CCDC 885972. For crystallographic data in CIF or other electronic format see DOI: 10.1039/c3cc00244f



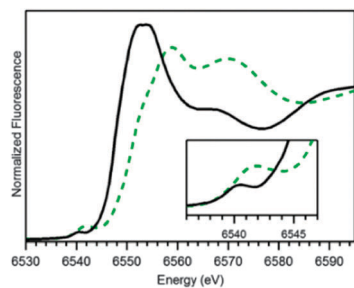


**Fig. 2** 20 K Mn K-edge XAS near-edge region of **1**(OTf)<sub>2</sub> (black solid trace) and **2** (green dashed trace) in H<sub>2</sub>O and CF<sub>3</sub>CH<sub>2</sub>OH, respectively.

of **2** (6550.8 eV) is blue-shifted over 3 eV relative to that of **1**, as expected for the higher oxidation state of Mn (Fig. 2). The edge energy of **2** is within 1 eV of those reported for Mn<sup>IV</sup>=O complexes supported by salen and porphyrin ligands (6549.9–6551.2 eV; Table S3; ESI<sup>†</sup>).<sup>5</sup> The pre-edge peak of **2** at 6541.9 eV is significantly more intense than that of **1** (Fig. 2, inset), consistent with a large deviation from centrosymmetry.

The Fourier transform (*R'* space) of the EXAFS data of **2** exhibits a prominent, sharp peak at *R'* ≈ 1.5 Å with less prominent peaks at *R'* ≈ 1.9, 2.2, and 2.8 Å (Fig. 1C). The first coordination sphere of **2** is fit well with two or three shells of N/O atoms at distances (*r*) of 1.69, 2.00, and 2.24 Å (Table S4; ESI<sup>†</sup>). The shell at 1.69 Å, which corresponds to the oxo ligand, is much shorter than the Mn<sup>II</sup>–O (solvent H<sub>2</sub>O) distance of 2.09 Å observed for **1**. The remaining first coordination sphere can be fit with either a single shell of 5 nitrogen scatterers at 1.99 Å or two shells of nitrogen scatterers at 2.00 Å (4 N atoms) and 2.24 Å (1 N atom), representing the nitrogen atoms of the pentadentate N4py ligand. The fit with two shells of N scatterers affords lower GOF and Debye–Waller values than the fit with just one shell of five N scatterers. Fits including outer-sphere features reveal two Mn···C shells at 2.82 and 2.97 Å (3 and 5 C atoms, respectively).

Metric parameters from the EXAFS data of **2** are in good agreement with a DFT-computed structure (Fig. 1A, right). This structure has a Mn=O bond of 1.673 Å (*cf.* the EXAFS distance of 1.69 Å). The equatorial nitrogens in the DFT-optimized structure have an average Mn–N distance of 2.024 Å, while the *trans* amine has a longer distance of 2.138 Å, consistent with the two shells of Mn–N scatterers at 2.00 and 2.24 Å.

The ability of **2** to activate C–H bonds was investigated using dihydroanthracene (DHA), diphenylmethane (DPM), ethylbenzene (EtBz), and toluene (Tol), which span a ~10 kcal mol<sup>-1</sup> range of C–H bond strengths. For each substrate, the addition of an excess to **2** at 298 K under an Ar atmosphere led to (i) a disappearance in the optical bands of **2**, (ii) formation of a new species, **3**, with bands at 460 and 630 nm, and (iii) the appearance of an isosbestic point at 714 nm (Fig. 3A). The decay of **2** and the formation of **3** occurred with the same rate, both following pseudo-first order behaviour to at least four half-lives (see ESI<sup>†</sup>). Second-order rate constants (*k*<sub>2</sub><sup>'</sup>, corrected for the number of reactive C–H bonds) determined for all substrates revealed a linear relationship between log(*k*<sub>2</sub><sup>'</sup>) and substrate bond dissociation enthalpies (BDEs), with a slope of 0.35 (Fig. 3B). Such behaviour is highly suggestive of a rate-limiting H-atom transfer.<sup>3a</sup> In support, reactions of **2** with deuterated-DHA (d<sub>4</sub>-DHA) reveal a kinetic isotope effect (KIE) of 11.2, which is larger than that observed for DHA

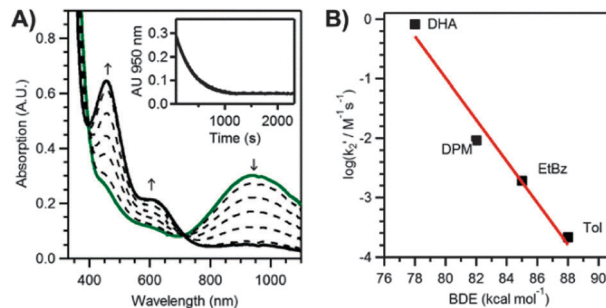


**Fig. 3** (A) Electronic absorption spectra of **2** upon addition of 200 equiv. EtBz in CF<sub>3</sub>CH<sub>2</sub>OH at 298 K. Inset: decay of the 950 nm absorption signal. (B) Corrected second-order rate constant (*k*<sub>2</sub><sup>'</sup>) versus bond dissociation enthalpies of organic substrates.

oxidation by other Mn<sup>IV</sup>=O adducts (3.1–8).<sup>2c,3a,4a,9</sup> Activation energies (*E*) and Arrhenius prefactors (*A*) determined from the reaction of **2** with DHA and d<sub>4</sub>-DHA from 35 to –5 °C in 1 : 1 CF<sub>3</sub>CH<sub>2</sub>OH : CH<sub>2</sub>Cl<sub>2</sub> provide evidence for H-atom tunnelling (Table S10; ESI<sup>†</sup>). Specifically, the difference in activation energies for DHA and d<sub>4</sub>-DHA (*E*<sub>D</sub> – *E*<sub>H</sub>) is greater than the difference in zero-point energies of the C–H and C–D bonds (3.6 and 1.26 kcal mol<sup>-1</sup>, respectively); and the ratio of Arrhenius prefactors (*A*<sub>H</sub>/*A*<sub>D</sub> = 0.02) is much less than 0.7, and comparable to that of [Fe<sup>IV</sup>(O)(N4py)]<sup>2+</sup>, where a H-atom tunnelling mechanism was also implicated.<sup>10</sup> The reaction of **2** with DHA proceeded with a second-order rate constant (*k*<sub>2</sub><sup>'</sup> = 3.6 M<sup>-1</sup> s<sup>-1</sup>) 2–3 orders of magnitude larger than those observed at similar temperatures for nearly all other non-porphyrinic Mn<sup>IV</sup>=O complexes (Table S8; ESI<sup>†</sup>).<sup>3a,4a,9,11</sup> An Eyring analysis of DHA activation from 35 to –5 °C, reveal Δ*H*<sup>‡</sup> and Δ*S*<sup>‡</sup> of 9 ± 0.8 kcal mol<sup>-1</sup> and –35 ± 3 cal mol<sup>-1</sup> K, respectively (Table S9; ESI<sup>†</sup>). These parameters yield a Δ*G*<sup>‡</sup> (at 25 °C) comparable to that of [Mn<sup>IV</sup>(O)(H<sub>3</sub>buea)]<sup>–</sup> but 2 kcal mol<sup>-1</sup> smaller than those observed for other Mn<sup>IV</sup>=O complexes,<sup>3a,4a,b</sup> consistent with the greater reactivity of **2**.

The reaction of **2** with DHA yielded 0.56(8) equiv. of anthracene per equiv. of **2**. A final Mn oxidation state of 2.7(15) was determined by iodometric titration. This product distribution is consistent with the generation of anthracene by reaction of 1 equiv. DHA with 2 equiv. Mn<sup>IV</sup>=O rather than two successive H-atom transfers with a single Mn<sup>IV</sup>=O centre. Thus, **2** acts as a one-electron oxidant, which has been observed for other Mn<sup>IV</sup>=O compounds.<sup>2c,3a,b,4c</sup> Such reactivity is consistent with DFT studies by Shaik and Nam that have shown a second H-atom transfer between the nascent organic radical and Mn<sup>III</sup>–OH centre to be less favorable than diffusion of the organic radical from the Mn<sup>III</sup>–OH adduct.<sup>12</sup> To the best of our knowledge, two-electron oxidation of DHA by a Mn<sup>IV</sup>=O has only been observed for [Mn<sup>IV</sup>(O)<sub>2</sub>(Me<sub>2</sub>EBC)]<sup>+</sup> and [Mn<sup>IV</sup>(O)(OH<sub>2</sub>)(BQCN)]<sup>2+</sup>.<sup>3c,4c</sup>

While the iodometric product analysis gives an average Mn oxidation state following the reaction of **2** with DHA, the nature of the Mn-based products can be better defined on the basis of EPR, electronic absorption, and ESI-MS data. Perpendicular-mode EPR spectra of the product solution showed the strong Mn<sup>IV</sup>=O signals replaced by very weak signals. Broad features over a large field range and a sharp multiline signal at *g* ≈ 2 are respectively attributed to mononuclear Mn<sup>II</sup> and binuclear species (Fig. S5; ESI<sup>†</sup>). Corresponding parallel-mode EPR spectra are silent. This does not preclude the presence of mononuclear Mn<sup>III</sup> species,



as favourable  $\text{Mn}^{\text{III}}$  zero-field splitting parameters and high-quality glasses are often required to observe the weak six-line signals of mononuclear  $\text{Mn}^{\text{III}}$  centres in X-band experiments. The optical absorption features of product **3** are quite similar to those of  $[\text{Mn}^{\text{III}}(\text{OCH}_2\text{CF}_3)(\text{Bn-TPEN})]^{2+}$  ( $\text{Bn-TPEN} = N\text{-benzyl-}N,N',N'\text{-tris-(2-pyridylmethyl)-1,2-diaminoethane}$ ), which was the dominant Mn product when  $[\text{Mn}^{\text{IV}}(\text{O})(\text{Bn-TPEN})]^{2+}$  was reacted with hydrocarbons.<sup>3b</sup> In addition, the dominant molecular ion peak in ESI-MS data of **3** is at  $m/z$  620.1289, consistent with  $[\text{Mn}^{\text{III}}(\text{OCH}_2\text{CF}_3)(\text{N4py})][\text{OCH}_2\text{CF}_3]^+$  ( $m/z$  calc. 620.1293). Thus, we propose a mononuclear  $\text{Mn}^{\text{III}}$  species as the dominant, but not sole, Mn-based product when **2** reacts with DHA.<sup>13</sup>

The chemical reactivity of **2** is similar to that of  $[\text{Mn}^{\text{IV}}(\text{O})(\text{Bn-TPEN})]^{2+}$ .<sup>3b</sup> Both N4py and Bn-TPEN are N5 aminopyridyl ligands that also support highly reactive  $\text{Fe}^{\text{IV}}=\text{O}$  complexes.<sup>10</sup> For the  $\text{Mn}^{\text{IV}}=\text{O}$  adducts, previous DFT computations predicted that **2** has a larger barrier for H-atom abstraction from cyclohexane than  $[\text{Mn}^{\text{IV}}(\text{O})(\text{Bn-TPEN})]^{2+}$ .<sup>12</sup> Although the addition of a large excess (400–600 equiv.) of cyclohexane increases the decay rate of **2**, the reaction does not show pseudo-first order behaviour. In contrast,  $[\text{Mn}^{\text{IV}}(\text{O})(\text{Bn-TPEN})]^{2+}$  reacts with cyclohexane at 25 °C. Thus, we are unable to determine a  $k_2$  value to provide a quantitative comparison of reactivity using cyclohexane. However, a comparison can be made using EtBz, with which both compounds react at 25 °C in  $\text{CF}_3\text{CH}_2\text{OH}$ . In the reaction with EtBz,  $[\text{Mn}^{\text{IV}}(\text{O})(\text{Bn-TPEN})]^{2+}$  (1 mM) shows a rate constant five-fold larger than that of **2** (2 mM):  $k_2' = 2.7 \times 10^{-2}$  and  $5.7 \times 10^{-3} \text{ M}^{-1} \text{ s}^{-1}$ , respectively. Thus, while **2** is dramatically more reactive towards C–H bonds than most  $\text{Mn}^{\text{IV}}=\text{O}$  adducts, it is less reactive than  $[\text{Mn}^{\text{IV}}(\text{O})(\text{Bn-TPEN})]^{2+}$ . This trend holds for the corresponding  $\text{Fe}^{\text{IV}}=\text{O}$  adducts; *i.e.*,  $[\text{Fe}^{\text{IV}}(\text{O})(\text{Bn-TPEN})]^{2+}$  is more reactive towards C–H bonds.<sup>10</sup>

The origin of the high reactivity of **2** towards C–H bonds is currently unclear. Cyclic voltammetry studies of **2** show a  $\text{Mn}^{\text{III/IV}}$  reduction potential ( $E_{1/2}$ )  $\sim 700$  mV higher than those of other  $\text{Mn}^{\text{IV}}=\text{O}$  complexes (ESI<sup>†</sup>).<sup>3a,4a,9</sup> Thus, **2** is a significantly more effective one-electron oxidant. Notably the  $E_{1/2}$  of **2** is similar to those of other dicationic  $\text{Mn}^{\text{IV}}$  complexes,<sup>3a,9</sup> suggesting that the increase in  $E_{1/2}$  is attributed to the +2 total charge of **2** versus the +1 and –1 charges of other  $\text{Mn}^{\text{IV}}=\text{O}$  adducts.<sup>3a,4a</sup> However, rates of H-atom transfer reactions, which are strongly correlated to thermodynamic driving force, depend not only on the reduction potential of the oxidant, but also on the basicity of the metal-hydroxo product.<sup>14</sup> Both the  $\text{Mn}^{\text{III/IV}}$  reduction potential and the  $\text{p}K_a$  of the  $\text{Mn}^{\text{III}}\text{-OH}$  complex, which for this system is unknown, are necessary for a thermodynamic analysis. While we cannot comment at present on the driving force for C–H bond activation by **2**, we note that many other  $\text{Mn}^{\text{IV}}=\text{O}$  adducts have sterically demanding supporting ligands that shield the oxo. In contrast, the oxo ligand in **2** is well-exposed to substrate (Fig. 1A). Reduced steric clash with substrate could contribute to the relatively high reactivity of **2**. Future work is needed to determine the role ligand sterics, solvent effects, and thermodynamic driving force play in influencing the H-atom transfer reactivity of **2**, and to explore further why  $\text{Mn}^{\text{IV}}=\text{O}$  adducts such as **2** may eschew standard rebound or desaturation mechanisms for C–H activation.

This work was supported by the US NSF (CHE-1056470 to T.A.J.; CHE-1004897 for R.I.; CHE-0946883 and CHE-0079282 supported instrument purchases). XAS experiments were supported by the Center for Synchrotron Biosciences grant, P30-EB-009998, from the National Institute of Biomedical Imaging and Bioengineering (NIBIB). We thank Dr Erik Farquhar at NSLS for outstanding support of our XAS experiments.

Most recently Chen *et al.* reported the formation and characterization of **2** and described the effects of  $\text{Sc}^{3+}$  on oxo and H-atom transfer reactions.<sup>12b</sup>

## Notes and references

- (a) J. P. McEvoy and G. W. Brudvig, *Chem. Rev.*, 2006, **106**, 4455–4483; (b) A. J. Wu, J. E. Penner-Hahn and V. L. Pecoraro, *Chem. Rev.*, 2004, **104**, 903–938; (c) R. Hage and A. Lienke, *Angew. Chem., Int. Ed.*, 2006, **45**, 206–222.
- (a) D. E. Lansky, A. A. Narducci Sarjeant and D. P. Goldberg, *Angew. Chem., Int. Ed.*, 2006, **45**, 8214–8217; (b) K. A. Prokop, S. P. de Visser and D. P. Goldberg, *Angew. Chem., Int. Ed.*, 2010, **49**, 5091–5095; (c) C. Arunkumar, Y.-M. Lee, J. Y. Lee, S. Fukuzumi and W. Nam, *Chem.–Eur. J.*, 2009, **15**, 11482–11489; (d) J. T. Groves, J. Lee and S. S. Marla, *J. Am. Chem. Soc.*, 1997, **119**, 6269–6273; (e) T. Taguchi, R. Gupta, B. Lassalle-Kaiser, D. W. Boyce, V. K. Yachandra, W. B. Tolman, J. Yano, M. P. Hendrich and A. S. Borovik, *J. Am. Chem. Soc.*, 2012, **134**, 1996–1999; (f) T. J. Collins and S. W. Gordon-Wylie, *J. Am. Chem. Soc.*, 1989, **111**, 4511–4513.
- (a) I. Garcia-Bosch, A. Company, C. W. Cady, S. Styring, W. R. Browne, X. Ribas and M. Costas, *Angew. Chem., Int. Ed.*, 2011, **50**, 5648–5653; (b) X. Wu, M. S. Seo, K. M. Davis, Y.-M. Lee, J. Chen, K.-B. Cho, Y. N. Pushkar and W. Nam, *J. Am. Chem. Soc.*, 2011, **133**, 20088–20091; (c) S. C. Sawant, X. Wu, J. Cho, K.-B. Cho, S. H. Kim, M. S. Seo, Y.-M. Lee, M. Kubo, T. Ogura, S. Shaik and W. Nam, *Angew. Chem., Int. Ed.*, 2010, **49**, 8190–8194; (d) T. H. Parsell, R. K. Behan, M. T. Green, M. P. Hendrich and A. S. Borovik, *J. Am. Chem. Soc.*, 2006, **128**, 8728–8729; (e) G. Yin, A. M. Danby, D. Kitko, J. D. Carter, W. M. Scheper and D. H. Busch, *J. Am. Chem. Soc.*, 2007, **129**, 1512–1513.
- (a) T. H. Parsell, M.-Y. Yang and A. S. Borovik, *J. Am. Chem. Soc.*, 2009, **131**, 2762–2763; (b) Y. Wang, S. Shi, H. Wang, D. Zhu and G. Yin, *Chem. Commun.*, 2012, **48**, 7832–7834; (c) S. Shi, Y. Wang, A. Xu, H. Wang, Z. Dajian, S. B. Roy, T. A. Jackson, D. H. Busch and G. Yin, *Angew. Chem., Int. Ed.*, 2011, **50**, 7321–7324.
- (a) K. Ayougou, E. Bill, J. M. Charnock, C. D. Garner, D. Mandon, A. X. Trautwein, R. Weiss and H. Winkler, *Angew. Chem., Int. Ed. Engl.*, 1995, **34**, 343–346; (b) T. Kurahashi, A. Kikuchi, T. Tosha, Y. Shiro, T. Kitagawa and H. Fujii, *Inorg. Chem.*, 2008, **47**, 1674–1686; (c) T. Kurahashi, A. Kikuchi, Y. Shiro, M. Hada and H. Fujii, *Inorg. Chem.*, 2010, **49**, 6664–6672.
- C. M. Hansel, C. A. Zeiner, C. M. Santelli and S. M. Webb, *Proc. Natl. Acad. Sci. U. S. A.*, 2012, **109**, 12621–12625.
- S. Chattopadhyay, R. A. Geiger, G. Yin, D. H. Busch and T. A. Jackson, *Inorg. Chem.*, 2010, **49**, 7530–7535.
- T. M. Rajendiran, J. W. Kampf and V. L. Pecoraro, *Inorg. Chim. Acta*, 2002, **339**, 497–502.
- G. Yin, A. M. Danby, D. Kitko, J. D. Carter, W. M. Scheper and D. H. Busch, *J. Am. Chem. Soc.*, 2008, **130**, 16245–16253.
- E. J. Klinker, S. Shaik, H. Hirao and L. Que, *Angew. Chem., Int. Ed.*, 2009, **48**, 1291–1295.
- A potential complication for this rate comparison is the difference in solvents (Table S8; ESI<sup>†</sup>). **2** reacts with DHA at essentially the same rate in 1 : 1  $\text{CF}_3\text{CH}_2\text{OH} : \text{CH}_2\text{Cl}_2$  (ESI<sup>†</sup>), though the KIE drops to 8.7. In other solvents **2** has limited stability or does not form.
- (a) K.-B. Cho, S. Shaik and W. Nam, *J. Phys. Chem. Lett.*, 2012, **3**, 2851–2856; (b) J. Chen, Y.-M. Lee, K. M. Davis, X. Wu, M. S. Seo, K.-B. Cho, H. Yoon, Y. J. Park, S. Fukuzumi, Y. N. Pushkar and W. Nam, *J. Am. Chem. Soc.*, 2013, DOI: 10.1021/ja312113p.
- In the absence of any substrate, the thermal decay of **2** yields a similar product, as judged by electronic absorption spectroscopy.
- J. M. Mayer, *Acc. Chem. Res.*, 2010, **44**, 36–46.

